Interdiffusion at Interfaces of Binary Polymer Mixtures with Different Molecular Weights

Woon Chun Kim and Hyungsuk Pak*

Department of Chemistry, Seoul National University, Seoul 151-742, Korea
Received May 25, 1999

Interdiffusion between two partially miscible polymers of similar chemical structures with different molecular weights is characterized theoretically by using the reptation model for the interdiffusion. This model provides more reliable results than the early Rouse model for same molecular weights, compared with the experiments. Furthermore, by introducing the molecular weight ratio R into the reptation model, we can see the dynamic effect of molecular weight on the diffusion behaviors of the asymmetric system. Near the critical point the diffusion behaviors of asymmetric binary polymer mixtures are well characterized by the interfacial width $W(t)$, the mass transport $M(t)$ for the different values of the Flory χ parameter and different molecular weight ratios of polymers of the diffusion couple. These two quantities and composition profiles by this model give better agreement with experiments.

Introduction

Interdiffusion of polymers is a problem of considerable interest for both basic knowledge and applications. Polymer/polymer interdiffusion affects the mechanical properties of polymers near interfaces. Applications include rubber-toughened polymer composites, welding of polymer interfaces, polymer adhension, and coating. Understanding of diffusion processes in polymers is a key to successful production of polymers and applications of polymer products in industry because the final properties of the polymer are determined by the thickness of the interface and the concentration profile of the two polymers across the interface. While mutual diffusion between miscible species is well understood,[1] little is known about the kinetics of diffusional mixing between immiscible or partially miscible materials. This is of particular relevance and has both basic and practical implications for the case of macromolecules, since most binary polymer pairs exhibit little compatibility at accessible temperatures.[2] Binary polymer mixtures are characterized by an upper critical solution temperature, and will segregate at lower temperatures into two coexisting phases separated by an interfacial region.[3] Recently, there has been a lot of interest in the interdiffusion of partly miscible and immiscible species. Typically, one prepares a thin film rich in one of the species (say A) and a second thin film rich in the other species (say B) is brought on top of it. The broadening of the initially sharp concentration profile in time is of considerable interest. The various experimental techniques have been developed for this purpose.[4-7] If polymers A and B are compatible, the initial sharp interface will be smeared out as a result of the ordinary Fickian type diffusion. But two different polymers in contact do not in general interdiffuse freely, and an interfacial zone of finite width separates them at equilibrium.[8-11] This incompatibility stems from a very low combinational entropy of mixing which scales inversely with the degree of polymerization N together with interactions between the different unfavorable monomers.[3] The unfavorable molecular interactions between unlike molecules are N independent and remain comparable to those of analogous small molecular mixtures.

Defining the interfacial width W as related to the reciprocal of the maximal composition gradient across the A B boundary, it was found that the thickness of the interface W increases with time slower than that of a Fickian process of $W(t) \propto t^{1/2}$. As the opposite of phase separation, the mixing takes place via interdiffusion driven by thermodynamic forces. The transport phenomena in the bilayer were found to depend strongly on thermodynamic conditions such as temperature, interaction parameters between polymers A and B, and molecular weights of A and B. A mean-field approach[12] suggests that the exponent α of a scaling law $W(t) \propto t^{\alpha}$ may be between ¼ and ½ near the critical temperature. Klein and co-workers have obtained the first direct measurement of time-dependent composition profiles at an interface between two partially miscible polymers A and B (deuterated and protonated polystyrene).[4,5] In the experiment of Klein and co-workers,[5] α was found considerably smaller than the Fickian exponent ½, falling between 0.25 and 0.5.

The value of α strongly depends on the definition by which the width W of the interface is measured. The definition of maximal gradient is most sensitive to the local structure of interface. A second meaningful characterization of interdiffusion is defining the amount of material $M(t)$ of species A transported across the interface separating A and B as a function of time: $M(t) \propto t^{\beta}$. This definition is most insensitive to the local structure of the composition profile. Interdiffusive behaviors of polymer mixtures can be characterized by following interfacial width, mass transport across the interface. Thus, we consider interdiffusion between *pure* polymer A and *pure* polymer B assuming the polymer layers are infinitely thick. Here, by using the *reptation* model for the interdiffusion, we study theoretically the binary polymer mixtures of similar (not same) chemical structure ($\chi > 0$)

with *different* molecular weights, and better agreement is found than the early Rouse model[13] for same molecular weights if it is compared with experiments.[4,5,6,24]

Theory of Polymer Interdiffusion

A spatially homogeneous polymer mixture consisting of two polymer components A and B can be described approximately by the mixing-free-energy function $f(\phi)$ which is defined as follows according to the so-called mean-field theory. For the sake of simplicity, we consider the case that the volume of the mixture does not change upon mixing. The function $f(\phi)$ is defined as the free energy per unit volume of the mixture. In the mean field theory for incompressible polymer mixtures of lengths N_A and N_B, $f(\phi)$ is given by

$$f(\phi) = \frac{\phi}{N_A}\ln(\phi) + \frac{1-\phi}{N_B}\ln(1-\phi) + \chi\phi(1-\phi) \qquad (1)$$

where ϕ is the volume fraction of A and χ is the Flory-Huggins parameter.[3,14]

The first two terms in Eq. (1) describe the combinatorial entropy while the third term accounts for segment-segment interaction energy. Since N_A and N_B are large and the entropy of mixing is small, the thermodynamic driving force for mixing is very weak and a relatively small positive Flory χ parameter is sufficient to make A and B phase-separate into A-rich and B-rich phases. For most A-B polymer pairs, χ is positive and larger than χ_c (critical value of χ for segregation), and segregation occurs. When the mixture phase-separates, interfaces are created between two phases. At phasic boundaries, polymers rearrange their conformations and repel chains of dissimilar species. This leads to an increase in free energy of both entropic and enthalpic origins. Let us now consider the case where the composition is not uniform. In this case, the free energy of the whole system can be described by the following form

$$F = \int dV\left[f(\phi(r,t)) + \frac{\kappa}{4}(\nabla\phi)^2\right] \qquad (2)$$

The first term represents the contribution from each volume element. The second term, which is referred to as the Cahn-Hilliard interfacial energy,[15,16] represents the cost of the free energy due to the presence of a concentration gradient when the composition is not uniform. The phenomenological parameter κ has the dimension of length squared and plays an important role in control and formation of interfaces.

In general, depending on the initial conditions, polymers A and B may either demix through spinodal decomposition or interdiffuse into each other. When the system is near the critical point for miscibility, mixtures cannot be perfectly phase-separated. In the same manner, polymers A and B will be partially mixed with each other *via* interdiffusion when pure A and pure B are put into contact. But the diffusion type will be different from the free-diffusion $t^{1/2}$ relation. By the thermodynamics the mixture cannot be mixed completely and a diffusion barrier exists. In our model, a sharp contact between two pure polymer layers A and B is arranged initially. The thermodynamic driving forces compel the system to mix through the interfacial region.

Mass conservation of polymer species A gives the following time evolution equation for ϕ:

$$\frac{\partial\phi}{\partial t} + \nabla\cdot J_A = 0 \qquad (3)$$

where the current is given by

$$J_A = -\Lambda(\phi)\nabla\mu \qquad (4)$$

In Eq. (4), $\Lambda(\phi)$ is a mutual mobility coefficient and depends on ϕ. The exchange chemical potential μ, which is functional derivative of the free energy F given in Eq. (2),

$$\mu(r) = \frac{\delta F}{\delta\phi(r)} \qquad (5)$$

To derive the functional form of $\Lambda(\phi)$ at a phenomenological level, we set the off-diagonal Onsager coefficients due to the hydrodynamic interaction to zero.[17] The cross-coefficient or the Onsager coefficient of component A due to the gradient of component B is only important in systems with electrostatic interactions. For interdiffusion in polymer pairs without ionic groups such as PVC/PMMA or PS/PVME, the cross-coefficients can be neglected.[7] Thus, for highly entangled linear polymers A and B,

$$\Lambda_A = \phi\Lambda_0\frac{N_e}{N_A},\quad \Lambda_B = (1-\phi)\Lambda_0\frac{N_e}{N_B} \qquad (6)$$

where Λ_0 is a monomer mobility and N_e is the entanglement degree of polymerization for the polymers ($N_A, N_B >> N_e$).[17] We here assume that the polymers A and B have same monomer mobility Λ_0. In this case, $\Lambda(\phi)$ takes the form

$$\Lambda(\phi) = \frac{\Lambda_A\Lambda_B}{\Lambda_A - \Lambda_B} = \frac{\phi(1-\phi)\Lambda_0 N_e}{N_A\{(1-\phi)+R\phi\}} \qquad (7)$$

where R (N_B N_A) represents the molecular weight ratio and Λ_0 is assumed to be independent of $\phi(r,t)$.

The equilibrium theory[8,10,23] for the interfacial structure of incompatible polymer blends also produces a simple expression for the parameter $\kappa(\phi)$ in Eq. (2) as

$$\kappa(\phi) = \frac{\sigma_A^2}{\phi} + \frac{\sigma_B^2}{(1-\phi)} = \frac{a^2}{\phi(1-\phi)} \qquad (8)$$

where σ_A, σ_B, assumed to be independent of ϕ, are segment lengths of polymers A and B respectively. In Eq. (8), we let $\sigma_A = \sigma_B = a$ where a is the characteristic length.[11] This is almost true in the system which consists of protonated and deuterated polymers of the identical chemical structure. Eqs. (1)-(5) and (7) constitute the dynamic model for spinodal decomposition in polymer blends, first proposed by de Gennes.[9,11] Now, the local chemical potential difference $\mu(r,t)$ is given by a functional derivative as usual

$$\nabla\mu(r,t) = \nabla\frac{\delta F}{\delta\phi(r,t)} = \frac{1}{N_A}\left(\frac{\nabla\phi}{\phi}\right) + \frac{1}{N_B}\frac{\nabla\phi}{1-\phi} - 2\chi\nabla\phi - \frac{a^2}{2}\frac{\nabla^3\phi}{\phi(1-\phi)} \qquad (9)$$

In arriving at Eq. (9), we have neglected nonlinear terms involving $(\nabla\phi)^3$ and $(\nabla\phi)\nabla^2\phi$. These terms are unimportant at late stages of interdiffusion when the interface has sufficiently broadened. Combining Eq. (4) and Eq. (7) with Eq. (9), the flux J_A of species A across a plane fixed with respect to the initial sharp interface is obtained:

$$J_A = -\frac{\phi(1-\phi)\Lambda_0 N_e}{N_A\{(1-\phi)+R\phi\}}\nabla\mu \tag{10}$$

where D_A ($\Lambda_0 N_e N_A^{-2}$) is the self-diffusion coefficient of highly entangled linear polymer A in melt and K ($=N_A a^2$) has the magnitude of the square of the end-to-end distance in an unperturbed chain.

Like the interdiffusion taking place between two thin sheets of polymers A and B, let us consider a one dimensional transport along the x-axis normal to the plane of sheet. We write our model in dimensionless form via scaling length and time. The length is scaled by the natural length $K^{1/2}$ and made conversion $x \rightarrow x K^{1/2}$ and the time is scaled with the unit τ $2K/D_A$, which is on the order of the reptation time of a single chain in a melt, and made the transformation $t \rightarrow t\ \tau$. Finally the composition variable is redefined as ψ $2(\phi - 1/2)$ so that the order parameter ψ takes values between +1 (pure A) and −1 (pure B) as composition profile ϕ drops from 1 to zero, and we have also made a change of notation: $N_A\chi \rightarrow \chi$ where $\chi_c = 2$ in the critical point of the symmetric case (R = 1). The resulting equation in terms of the rescaled variables is given by

$$\frac{\partial\psi}{\partial t} = \frac{\partial}{\partial x}\left\{\left(\frac{2}{1+R+(R-1)\psi}\right)\left(\left\langle 1+\frac{1}{R}-\chi+\left(\frac{1}{R}-1\right)\psi+\chi\psi^2\right\rangle\frac{\partial\psi}{\partial x}-\frac{\partial^3\psi}{\partial x^3}\right)\right\} \tag{11}$$

The factor in front of $\partial\psi/\partial x$ in Eq. (11) describes a diffusion coefficient which represents N^{-2} dependence in the reptation model. The second term involving $\partial^3\psi/\partial x^3$ accounts for the presence of an interface separating two incompatible phases and moderates the structure formation because too steep gradients are thermodynamically disadvantageous.

Computational Methods

Eq. (11) is a non-linear equation for ϕ, and solving it generally requires numerical computation obtained by discretizing Eq. (11) with finite differences. Let us consider a bilayer of initially pure polymer A and polymer B where the left-hand side is occupied by A and the right-hand side by B. The evolution of the bilayer system starting from the initial profile of a step function is described by application of the standard Crank-Nicholson method to update at every time step the profile described by Eq. (11). We discretize $\partial\psi(x,t)/\partial t$ as $(\psi_i^{n+1}-\psi_i^n)/\Delta t$, $\partial\psi(x,t)/\partial x$ as $(\psi_{i+1}^n-\psi_{i-1}^n)/2\Delta x$, and similarly for its higher spatial derivatives with $\Delta t = 0.01$ and $\Delta x = 0.5$. The total grid points are 700, so that the total thickness is 350 $K^{1/2}$. We take the initial interface of the bilayer system as $350\Delta x$ (=175 $K^{1/2}$). The boundary conditions to solve the above diffusion equation are $\partial\psi(x,t)/\partial x$ 0 and $\partial^3\psi(x,t)/\partial x^3 = 0$ at the outer two ends of the bilayer. Then, the system is allowed to evolve 10^5 time steps (= $10^3\tau$) with an initial interfacial width of a reasonable magnitude as long as the boundary condition will remain valid.

A quantitative measure for the interfacial broadening is the interfacial width $W(t)$ defined as the inverse of the slope at the point of the interface where the composition profile $\psi(x)$ varies most rapidly:

$$W(t) = \left[\left(\frac{\partial\psi(x,t)}{\partial x}\right)_{\max}^{-2} - \left(\frac{\partial\psi(x=350\Delta x,t=0)}{\partial x}\right)^{-2}\right]^{-1/2} \tag{12}$$

where $W(t)$ is given in units of $K^{1/2}$. We take $W(0)$ considerably smaller than $W(\infty)$ to start the interdiffusion process on the computer. The mass transport $M(t)$ of polymer A transported from the left-hand side of the initial dividing surface to its right-hand side is calculated as

$$M(t) = C\int_{350\Delta x}^{700\Delta x} dx[1+\psi(x,t)] \tag{13}$$

where C is a proportionality constants. The mass transport depicts the overall profile of the composition field while the interfacial width reflects the local structure at the interface. It is expected that $M(t)$ will increase with time slower than $t^{1/2}$ for the partially miscible couples of polymer blends because of the suppressed diffusion due to the "spinodal barrier".

We have considered three values of χ = 1.6, 1.7, 1.8, and four values of R = 1, 1.5, 2.0, 3.0. In the Flory-Huggins mean field model of polymer mixing, χ_c is given by

$$\chi_c = \frac{(\sqrt{N_A}+\sqrt{N_B})^2}{2N_AN_B} \tag{14}$$

where χ_c is the value of χ at the critical temperature T_c. After we have made a change of notation $N_A\chi_c \rightarrow \chi_c$ and $N_B/N_A \rightarrow R$, the following expression for the Eq. (14) is obtained:

$$\chi_c = \frac{(1+\sqrt{R})^2}{2R} \tag{15}$$

In Eq. (15), $\chi_c = 2$ for the symmetric case (R = 1) and χ_c = 1.65, 1.46, 1.24 for R = 1.5, 2.0, 3.0, respectively.

Results and Discussion

Figure 1 shows the composition profiles of polymer A for A B diffusion couples which were diffused at χ = 1.6 for diffusion times, t, of 62, 250, 562, and 1000τ in R = 2. This figure shows that the composition profiles remain asymmetric as interdiffusion proceeds and the diffusion behaviors differ significantly from those for the symmetrical case.[13] All the composition profile curves appear to intersect at a single point at the original interface. This means that the number of chains per unit area crossing the original interface instantaneously reaches a constant value after a short reptation time.[26] As we see in Figure 1, the lower molecular weight

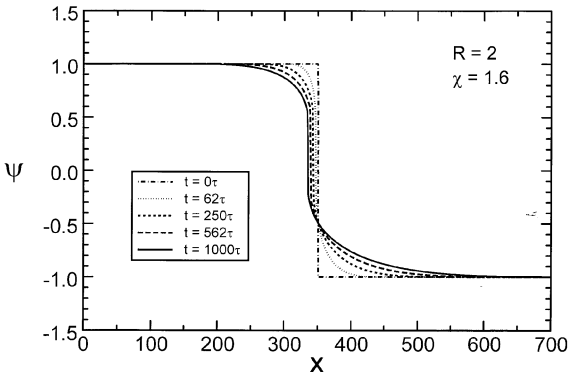

Figure 1. Time evolution of the composition profiles for χ 1.6 and $R = 2$ at five different times. $\chi_c = 1.46$ for $R = 2$. The time is expressed in units of $\tau(=2K D_0)$ and length in units of 0.5 $K^{1/2}$.

chains A diffuse more deeply into the high molecular weight B than the high molecular weight chains B diffuse into the low molecular weight side of the diffusion couple because of the entanglement effects. Therefore, Figure 1 demonstrates that the composition profiles do not vary smoothly with depth. It decreases rapidly with depth from pure A to a value around $\psi \leq -0.5$ but then much more slowly with depth as ψ decreases further. These behaviors are very similar to the experimental results of Figure 7 in ref 6 and Figure 4 in ref 25. The development of the interfacial width $W(t)$ for $R - 2$ at different values of χ (-1.6, 1.7, and 1.8) is monitored against the square root of the time and shown in Figure 2. Because binary polymer mixtures are characterized by an upper critical solution temperature, $\chi - 1.6$, 1.7, and 1.8 are away from the critical point ($\chi_c - 1.46$) toward one-phase region. Therefore, as the simulations of interdiffusion are carried out further away from the critical temperature which corresponds to $\chi_c - 1.46$ for $R - 2$, the transport behaviors seems to be more non-Fickian. The exact behaviors will be characterized in detail at the following figures. We see clearly how the interfacial width increases at short time but then levels off to its limiting value in Figure 2. A more detailed examination of the time variation indicates that, following an initial rapid increase, $W(t)$ varies as a power of t markedly slower than $t^{1/2}$, until it eventually levels out at its limiting value at sufficiently long times. These observations

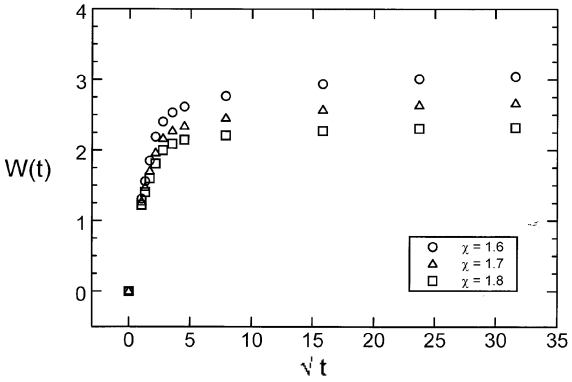

Figure 2. Interfacial width $W(t)$ against the square root of time for $\chi = 1.6$, 1.7, and 1.8 in $R = 2$. The units are the same as in Figure 1.

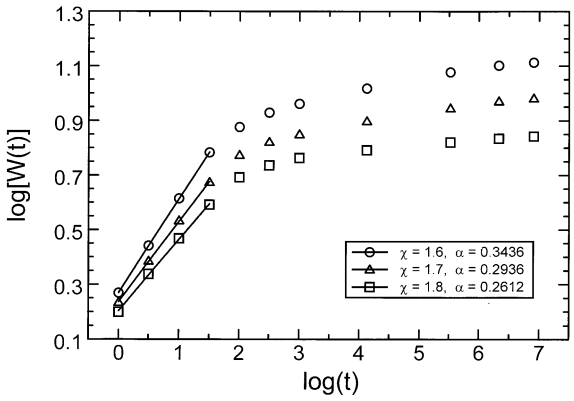

Figure 3. Natural log-log plots of the variation with time of the interfacial width for $\chi = 1.6$, 1.7, and 1.8 in $R = 2$. The solid lines are the linear fits that yield α.

emphasize the complexity of the interfacial development kinetics at $\chi > \chi_c$, and are in good agreement with the experimentally observed behaviors.[4,5] These can be more clearly investigated in greater detail by searching for the power-law relation: $W(t) \propto t^{\alpha}$. Figure 3 shows the development with time of $W(t)$ for $R - 2$ at three different values of χ, on a double-natural-logarithmic plot. We can see the power-law-like increase of $W(t)$ at short times, and leveling off to a constant value of $W(t)$ at long times. The initial variation of the interfacial width with time for $t \leq 4.48\tau$ ($\log [t] \leq 1.5$) is well represented by the power-law relation. This power variation is significantly different from the free-diffusion $\sqrt{t}$ relation. The solid lines in Figure 3 are the linear fits which yield the exponents α for the time development. The values of α are 0.3436, 0.2936 and 0.2612 for $\chi - 1.6$, 1.7 and 1.8, respectively. We note that α is in all three cases significantly smaller than the exponent 0.5 for free interdiffusion. Further away from the critical point given by $\chi_c - 1.46$, the larger χ value, the faster $W(t)$ saturates and the smaller α in Figure 3. These results are in good agreement with a mean-field approach[12] that, closer to the critical temperature, the expo-

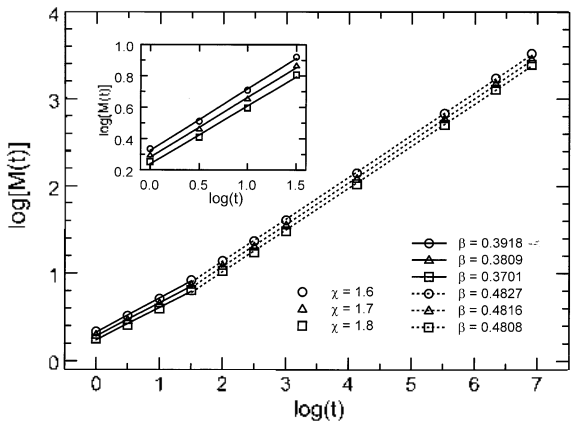

Figure 4. Natural log-log plots of the mass $M(t)$ transported across the initial dividing surface for R 2. The solid lines are the linear fits that yield β for $t < 4.48\tau$ ($\log[t] < 1.5$) and the details are given by inset. The dotted lines are the linear fits that yield β for $4.48\tau \leq t \leq 1000\tau$ ($1.5 \leq \log[t] \leq 6.91$)

an experiment.[5] Figure 4 shows the mass $M(t)$ transported across the initial dividing surface with time for $R = 2$ at three different values of χ, on a double-natural-logarithmic plot. The solid lines in Figure 4 are the linear fits that yield the β for $t \leq 4.48\tau$ ($\log[t] \leq 1.5$) and the details are shown in inset to Figure 4. The dotted lines are the linear fits that yield β for $4.48\tau \leq t \leq 1000\tau$ ($1.5 \leq \log[t] \leq 6.91$). The values of β in the solid lines are 0.3918, 0.3809 and 0.3701 for $\chi = 1.6$, 1.7, 1.8, respectively and 0.4827, 0.4816, 0.4808 in the dotted lines for the same each χ value. Still, the values of β stay within 0.25 and 0.5 but the values of β are greater than those of α. When we contrast two different quantities $W(t)$ and $M(t)$ that describe the same transport process, on the contrary, the mass transport $M(t)$ continues to increase with time without leveling off to its limiting value as shown in Figure 4. These contrasts of two quantities prove that the behaviors related to interfacial dynamics are significantly different from those concerned with mass transport. With more quantitative analysis by comparing α with β during the same initial period at three different values of χ, both values of α and β stay within 0.25 and 0.5. But, α decreases more steeply than β and the difference of two values increases, as χ grows larger. This explains that the exponent α is more sensitive to local structure of the interface and to the value of χ (~temperature) than the exponent β. Summing up, these come to the following result. The interfacial width $W(t)$ well characterizes the initial process of interdiffusion while the mass transport $M(t)$ well characterize the entire transport process and interdifussion in the late stage. From now, we will investigate the interdiffusion at the constant χ value (~temperature), varing the molecular weight ratio of the diffusion couple. The composition profiles of lower molecuar weight polymers A diffusing into higher molecular weight polymers B computed numerically for several molecular weight ratios of B to A at $t = 1000\tau$ and $\chi = 1.7$, are shown in Figure 5. The molecular weight ratio R ($=N_B/N_A$) is 1, 1.5, 2, and 3. As R becomes more than 1, the curves approach an asymptotic shape which is quite different from that obtained when $R = 1$ ($N_A=N_B$). As the length of polymer A is shorter than that of polymer B, the polymer A diffuse more deeply into the polymer B rich phase because of the chain entanglement in Figure 5. These shapes are similar to the simulated results of Figure 2 in ref 24. The development of $W(t)$ with time between coexisting homopolymer A-homopolymer B bilayers for $\chi = 1.7$ at different molecular weight ratios ($R = 1.5$, 2, and 3) is monitored and shown in Figure 6. The natural log-log plots of variation with time of the interfacial width at $\chi = 1.7$ for different values of R, are presented in Figure 7. The solid lines in Figure 7 are the linear fits that yield α for the initial period of time. The value of α is 0.3708, 0.2935 and 0.2638 for $R = 1.5$, 2 and 3 respectively. The mass transport $M(t)$ across the initial dividing surface for $\chi = 1.7$ is shown in Figure 8. The solid lines are also the linear fits that yield the β for $t \leq 4.48\tau$ ($\log[t] \leq 1.5$) and the details are given by inset to Figure 8. The dotted lines are the linear fits that yield β for $4.48\tau \leq t \leq 1000\tau$ ($1.5 \leq \log[t] \leq 6.91$). As expected, all the values of α and β are also between ¼ and ½ in Figure 7 and 8. As the value of R is larger than 1, diffusion behaviors are more non-Fickian and values of α and β are less than ½ of free-diffusion. However, β is less influenced by the molecular weight ratio R than α. Comparing Figure 7 with Figure 3, we are able to conclude that the interfacial width $W(t)$ is most sensitive to the local structure of the interface and much more affected by both the χ (~temperature) and the molecular weight ratio R, while the mass transport $M(t)$ is most insensitive to the local structure and much

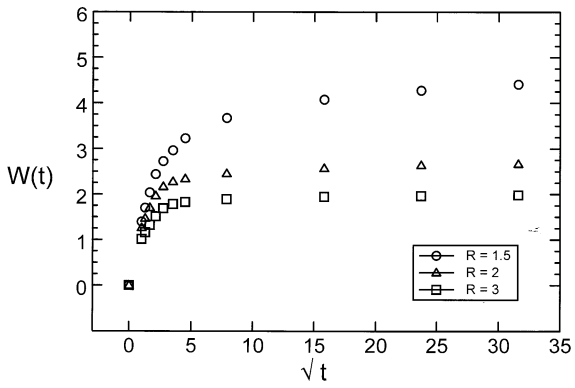

Figure 6. Interfacial width $W(t)$ against the square root of time for $R = 1.5$, 2 and 3 in $\chi = 1.7$. The units are the same as in Figure 1.

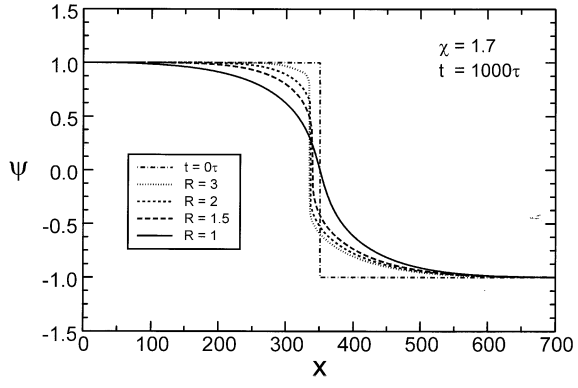

Figure 5. The composition profiles computed for N_B/N_A = 1, 1.5, 2, and 3 at $t = 1000\tau$ and $\chi = 1.7$. The units are the same as in Figure 1.

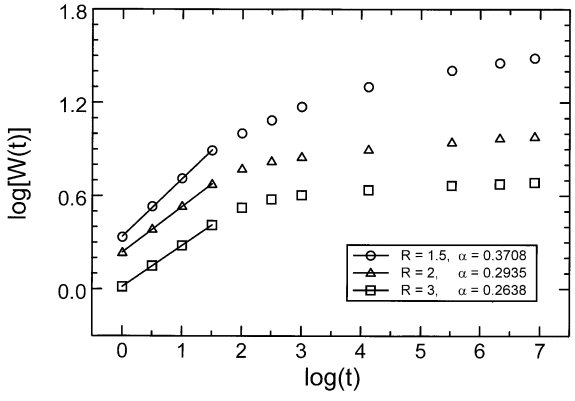

Figure 7. Natural log-log plots of variation with time of the interfacial width for χ = 1.7. The solid lines are the linear fits that yield α.

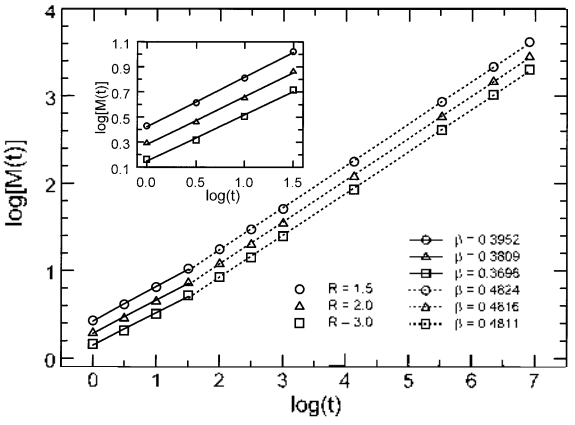

Figure 8. Natural log-log plots of the mass $M(t)$ transported across the initial dividing surface for $R = 1.5$, 2.0 and 3.0 in $\chi = 1.7$. The solid lines are the linear fits that yield β for $t \leq 4.48\tau$ ($\log[t] \leq 1.5$) and the details are given by inset. The dotted lines are the linear fits that yield β for $4.48\tau \leq t \leq 1000\tau$ ($1.5 \leq \log[t] \leq 6.91$).

less influenced by both χ and R. Furthermore, the interfacial width $W(t)$ can be used only in the early stage of the interdiffusion as a monitor of the interdiffusion process, while the mass transport $M(t)$ provides a characterization of the entire interdiffusion process including the late stage, in the asymmetric case ($R \neq 1$) as well as in symmetric case[13] ($R = 1$). In Figure 7 and 8, the values of α and β for $R = 1.5$ are 0.3708 and 0.3952 respectively and they are relatively close to 0.5 (free diffusion) because $\chi = 1.7$ is near the critical point for complete mixing ($\chi_c = 1.65$ for $R = 1.5$).

Conclusion

We have demonstrated that our model describes well the diffusion behaviors not only for *different* molecular weight ratio R at constant χ (−temperature) but also for different values of χ at fixed molecular weight ratio R ($\neq 1$), and our predictions agree well with available experimental data. Adopting the molecular weight ratio R ($=N_B/N_A$) and entanglement effect of mutual mobility into the symmetric Rouse model in ref 13, we can get the asymmetric diffusion behaviors of polymer mixture and obtain the dynamic effects of the molecular weight ratio R and the temperature ($-\chi$) on the interdiffusion through the interfacial width $W(t)$ and the mass transport $M(t)$. Therefore, we are able to study more exact behaviors of interdiffusion and more reliable comparison with experiments between two partially miscible polymer species with different molecular weights from a theoretical viewpoint. This model gives better description and agreement than the previous *Rouse* model[13] with *same* molecular weights in order to compare their model with experiments of *entangled* binary polymer mixtures with *different* molecular weights. In conclusion, our model can be well applied to the highly entangled binary polymer mixtures of deuterated and protonated species of the identical chemical structure with different molecular weights.

Acknowledgment. This research was supported by Basic Science Research Institute Program, Ministry of Education (BSRI-98-3414). We appreciate many useful discussions with Changjun Lee.

References

1. Doi, M.; Edwards, S. F. *The Theory of Polymer Dynamics*; Oxford Univ. Press: New York, 1986; Jones, R. A. L.; Klein, J.; Donald, A. M. *Nature* (London) **1986**, *321*, 161; Composto, R. J.; Mayer, J. W.; Kramer, E.; White, D. M. *Phys. Rev. Lett.* **1986**, *57*, 1312.
2. Olabisi, O.; Robenson, L. M.; Shaw, M. T. *Polymer-Polymer Miscibility*; Academic: New York, 1979.
3. de Gennes, P. G. *Scaling Concepts in Polymer Physics*; Cornell Univ. Press: Ithaca, New York, 1979.
4. Chaturvedi, U. K.; Steiner, U.; Zak, O.; Krausch, G.; Klein, J. *Phys. Rev. Lett.* **1989**, *63*, 616.
5. Steiner, U.; Krausch, G.; Schatz, G.; Klein, J. *Phys. Rev. Lett.* **1990**, *64*, 1119.
6. Composto, R. J.; Kramer, E. J. *J. Mater. Sci.* **1991**, *26*, 2815.
7. Jabbari, E.; Peppas, N. A. *Polymer* **1995**, *36*, 575.
8. Helfand, E.; Tagami, Y. *J. Chem. Phys.* **1972**, *56*, 3592.
9. de Gennes, P. G. *J. Chem. Phys.* **1980**, *72*, 4756; Pincus, P. *ibid.* **1981**, *73*, 1996.
10. Leibler, L. *Macromolecules* **1982**, *15*, 1283.
11. Binder, K. *J. Chem. Phys.* **1983**, *79*, 6387.
12. Harden, J. L. *J. Phys. (Paris)* **1990**, *51*, 1777.
13. Wang, S.-Q.; Shi, Q. *Macromolecules* **1993**, *26*, 1091.
14. Flory, P. J. *Principles of Polymer Chemistry*; Cornell Univ. Press: Ithaca, NY, 1953.
15. Cahn, J. W. *J. Chem. Phys.* **1963**, *422*, 93.
16. Cahn, J. W.; Hilliard, J. E. *J. Chem. Phys.* **1958**, *28*, 258.
17. Brochard, F.; Jouffory, J.; Levinson, P. *Macromolecules* **1983**, *16*, 1638.
18. Rouse, P. E. *J. Chem. Phys.* **1953**, *21*, 1273.
19. de Gennes, P. G. *Physics 3* **1967**, *3*, 37.
20. de Gennes, P. G. *J. Chem. Phys.* **1971**, *55*, 572.
21. Edwards, F.; Grant, J. *J. Phys.* **1973**, *A6*, 1169.
22. de Gennes, P. G. *J. Phys. (Paris)* **1981**, *42*, 735.
23. Helfand, E.; Sapse, A. M. *J. Chem. Phys.* **1975**, *62*, 1327.
24. Green, P. F.; Palmstrøm, C. J.; Mayer, J. W.; Kramer, E. J. *Macromolecules* **1985**, *18*, 501.
25. Shearmur, T. E.; Clough, A. S.; Drew, D. W.; van der Grinten, M. G. D.; Jones, R. A. L. *Polymer* **1998**, *39*, 2155.
26. Wu, S.; Chuang, H.; Han, C. D. *J. Polym. Sci. Polym. Phys. Ed.* **1986**, *24*, 143.